Numerical modeling of the Double Punch Test for plain concrete

Alba Pros[a], Pedro Díez[a], Climent Molins[b]

[a] *Laboratori de Càlcul Numèric*
Departament de Matemàtica Aplicada III
Universitat Politècnica de Catalunya, Barcelona Tech
Campus Nord UPC, 08034 Barcelona, Spain
e-mail: {alba.pros, pedro.diez}@upc.edu, web: http://www-lacan.upc.es
[b] *Departament d'Enginyeria de la Construcció*
Universitat Politècnica de Catalunya, Barcelona Tech
Campus Nord UPC, 08034 Barcelona, Spain
e-mail: climent.molins@upc.edu

Abstract

Double punch test is used to indirectly assess the tensile strength of plain concrete, f_t. For this normalized test, the tensile strength is obtained as a function of the failure load, P, which is expressed as $f_t = \mathcal{F}(P)$. Different authors have proposed different expressions for the relation $\mathcal{F}(\cdot)$, yielding scattered values of f_t. None of these alternatives is universally recognized as being more suitable than the others. In fact, these expressions are mainly based on elastic models considering the maximum tensile stress under the load P and f_t is obtained as an output of the linear model. A numerical simulation allows using models in which f_t is an input of the material model and the corresponding failure load P is obtained associated with each value of f_t. In the present work, double punch test is simulated numerically considering two alternatives for modeling plain concrete accounting for damage and cracking: (a) the nonlocal Mazars damage model and (b) an heuristic crack model including joint elements in an *a priori* defined crack pattern. Numerical results are validated with experimental data and compared with the analytical expressions available in the literature.

Keywords: Double Punch Test, Plain Concrete, Modeling, Numerical simulation, Finite Element Method, Nonlocal Mazars damage model, Fracture Mechanics, Joints, Validation

1. Introduction

The Double Punch Test (DPT) ([6, 8, 7]) is used to indirectly measure the tensile strength of plain concrete, f_t. Indirect measures of tensile strength (Brazilian test, DPT, 3 and 4 point bending test,...) are often preferred to direct uniaxial tests because (1) they are much easier to perform, particularly for controlling material production (for plain concrete, for example, the Brazilian test is of common and standard use) and (2) they show a reduced scattering of the results. The main focus of this work is proposing numerical models for the DPT in which f_t is an input parameter. The idea is to replace the naif linear elastic model by a more realistic one that has the tensile strength, f_t, already as one of material parameters and to identify the value of this material parameter that better fits the experimental results. These models are validated using experimental results and other analysis available in the open literature ([8, 3, 14, 17]).

The information extracted from the experimental tests is translated into the parameters characterizing the mechanical properties of the analyzed concrete. In this case, the parameter to be assessed is precisely the tensile strength, f_t. Essentially, the data provided by the experimental setup is a force-displacement curve in which the peak points corresponding to the collapse are easily identified. The force corresponding to the peak point, P, is readily translated into the tensile strength value using a theoretical model simulating the mechanical behavior of the test, $f_t = \mathcal{F}(P)$. Currently, the underlying theoretical model used in this framework is an analytical solution of the linear elastic problem [4, 5]. These models are a crude approximation of the actual behavior of the specimen close to the collapse regime but they still provide a good approach to the tensile strength by selecting a characteristic tensile stress in the linear elastic solution for the peak force, P.

Two different approaches are considered in order to model the mechanical behavior of the concrete in the DPT. Firstly (option A), a continuous model which has been successfully used modeling the common Brazilian test [19], the nonlocal Mazars damage model ([15, 1, 10, 18, 19]). Secondly (option B), a model which introduces discontinuous fracture at the surfaces corresponding to an *a priori* defined cracking pattern, based on the experimentally observed fracture mechanisms ([9, 2, 20]). On the fracture surfaces, joint elements with cohesive dilatant behavior are used to model the interfaces. In the rest of the specimen, the mechanical behavior is assumed to be linear elastic because the relevant deformation is concentrated in the fracture sur-

faces. Here, 3D finite element approximations are used complemented (for option B) with 2D joint elements. Both options A and B are solved using 3D finite elements.

Both options A and B provide approximations of the pre-peak and the post-peak behavior. Therefore, the information that may be extracted from the numerical tests is very rich and, in addition, to identify the parameters it may allow gaining further knowledge on the phenomenon.

The goal of this study is to analyze the features of the different models and their capabilities to properly approximate the experimental tests by fitting the experimental data available. An objective comparison is performed by setting a measure of the error between the experimental data and the model, this is equivalent to define a fitting criterion. Correspondingly, the parameter identification and the model validation are carried out both based on the same criterion.

All the experimental results are from an experimental campaign which consisted of the characterization of an specific concrete, including the double punch test. Hence, experimental data is available not only from the double punch test, but also from two different tests.

Thus, sophisticated models are used to identify the tensile strength from the DPT, instead of the linear elastic model. The advantage of using this approach is more relevant when DPT is used to identify the tensile behavior of steel fiber reinforced concrete. For fiber reinforced concrete (FRC), taking into account the post-peak behavior (and not only the peak) is extremely relevant. The present work has to be seen as a first step towards including steel fibers into these models in order to simulate the extension of the DPT to assess the after cracking capacity of FRC (a test introduced in [17, 16], named as the *Barcelona Test*).

The remainder of this paper is structured as follows. First, in section 2 the double punch test is presented, the problem statement is defined and the analytical expressions relating the tensile strength and the value of the maximum vertical load ($f_t = \mathcal{F}(P)$) are introduced, as well as the experimental campaign. Section 3 presents the numerical simulation: the continuous model and the discontinuous one. Then, in section 4, the numerical results are presented and contrasted. Moreover, the numerical results are validated with the experimental and analytical results available. Finally, the most important conclusions are listed.

2. Double Punch test

2.1. Description of the Double Punch Test

Double punch test was introduced in [6, 8, 7] as a tool to assess indirectly the tensile strength of plain concrete. It was presented as an alternative to the Brazilian test, which was so far the most common indirect tension test.

The test layout is illustrated in figure 1 and consists in compressing axially a cylindrical concrete specimen with two steel circular punches centered at the top and the bottom of the specimen. The geometry of the specimen is given by the height ($l = 15$cm) and the diameter ($d = 15$cm). The ratio between the diameters of the punches and the specimen is one fourth ($d' = \frac{1}{4}d = 3.75$cm). Occasionally, smaller specimens with identical geometrical proportions are used to study the influence of size effect ([8]), concluding that the tensile strength interpreted from the DPT is relatively insensitive to the size of the specimen.

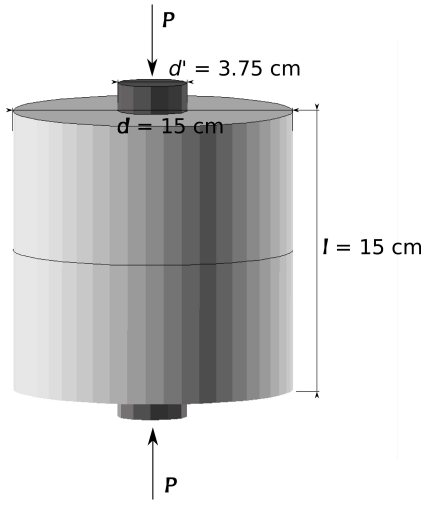

Figure 1: Double Punch Test layout

A typical failure mechanism presents three radial fracture planes. However, in the experimental results, the observed number of fracture planes ranges from two to four. The geometry of the collapse pattern is completed with two fracture cones beneath each punch. In figure 2 two different fracture patterns are illustrated.

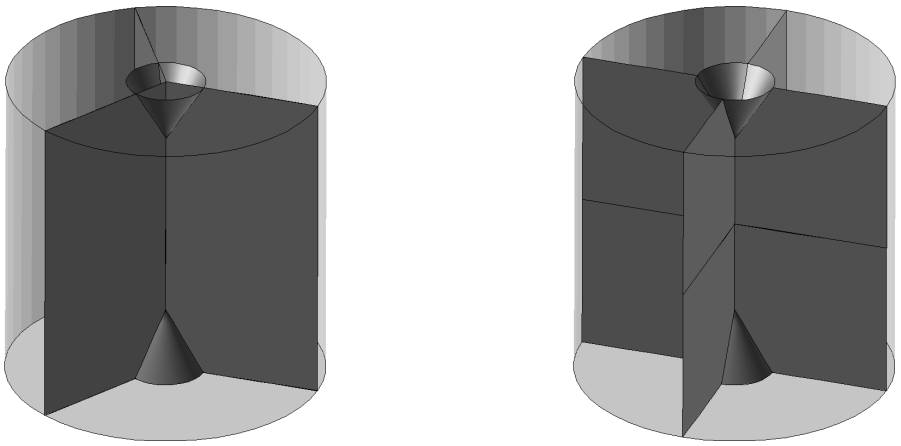

Figure 2: Two possible collapse mechanisms with three and four radial fracture planes

The goal of the present simulations is to describe the collapse of the specimen, with special interest in determining the peak load. Describing the chronological sequence of the cracks appearance, as discussed in [11, 12], is beyond the scope of this paper. In the models used here the fracture pattern is such that the specimen is partitioned into blocks that behave as rigid-bodies. Thus, the kinematics compatibility of the motion of these blocks undergoes a simultaneous development of the two basic mechanisms, namely the cone penetration and the separation of the crack planes.

The classical indirect tension test for plain concrete is the Brazilian test. DPT is often preferred to the Brazilian test because it is easier to carry out and the tensile strength is sampled in different cracked planes and, therefore, the quantity obtained corresponds to an average. On the contrary, the Brazilian test confines failure to a predetermined plane. Moreover, for Steel Fiber Reinforced concrete DPT captures better fibers influence than Brazilian test, due to their fracture mechanisms.

The experimental set up is a displacement controlled compression at a velocity of 0.5mm/min.

2.2. Close-form expressions for tensile strength determination

Some analytical expressions of the tensile strength are available in the literature for the DPT. The maximum compression load (P) and the dimensions of the test (d, d' and l) are the inputs in each analytical expression.

Chen and Yuan [8] applied a limit analysis idealizing concrete as a linear elastic-perfectly plastic material with very large ductility obtaining

$$f_t = \frac{P}{\pi(1.2\frac{d}{2}l - (\frac{d'}{2})^2)}. \tag{1}$$

Moreover, in order to be more accurate, they carried out a finite element analysis considering concrete as an elastic plastic strain-hardening and fracture material and the final expression proposed is

$$f_t = \frac{0.75P}{\pi(1.2\frac{d}{2}l - (\frac{d'}{2})^2)}. \tag{2}$$

However, there are other analytical approximations of the tensile strength in the DPT given by different authors as follows.

Based on a nonlinear fracture mechanics approach, Marti [14] proposed

$$f_t = 0.4\frac{P}{4(\frac{d}{2})^2}\sqrt{1 + \frac{d}{\lambda d_a}} \tag{3}$$

where d_a is the maximum aggregate size and λ is an experimental parameter depending on the material. This expression is given in order to analyze the size effect of the specimen on the tensile strength value.

In [3], Bortolotti assumed a modified Coulomb-like failure criterion for concrete getting

$$f_t = \frac{P}{\pi(\frac{d}{2}l - (\frac{d'}{2})^2 \cot\alpha)} \tag{4}$$

considering $\alpha = \frac{\pi}{2} - \frac{\phi}{2}$ with ϕ being the internal friction angle in the modified Coulomb's yield criterion.

Finally, Molins et al. [17], presented another analytical expression based on limit analysis,

$$f_t = \frac{P}{9\pi l\frac{d'}{2}}. \tag{5}$$

In the following, these expressions are used for comparision purposes and we restrict ourselves to the expressions given in equations (1), (2) and (5).

2.3. Experimental campaign

The DPT is contrasted with two standard tests (the uniaxial compression test and the Brazilian test). The set up of these two tests is recalled bellow.

2.3.1. Uniaxial compression test

The specimen of the uniaxial compression test, presented in figure 3, is a concrete cylinder of size $l = 30$ cm and $d = 15$ cm. The compression load is uniformly distributed at the top and bottom of the specimen.

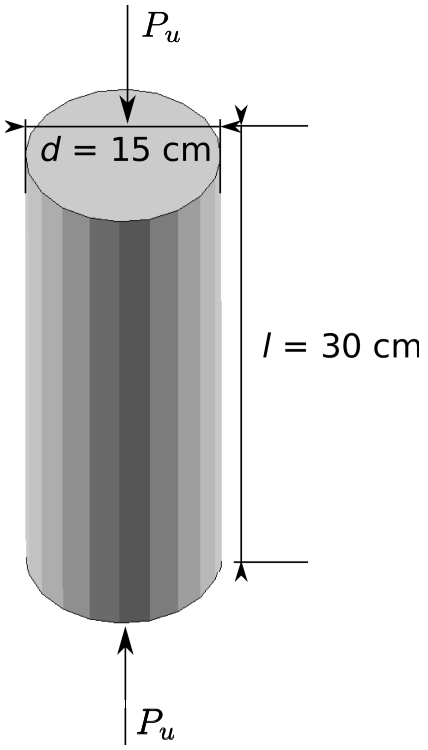

Figure 3: Description of the uniaxial compression test

This is a direct compression test which provides the compressive strength, f_c. The relationship between the compressive strength f_c and the maximum vertical load P_u is given by

$$f_c = \frac{4P_u}{\pi d^2} \tag{6}$$

where d stands for the diameter of the specimen.

Experimentally, the value obtained is $P_u = 8.9 \cdot 10^5$N, which is translated into f_c through equation (6): $f_c = 50.45$MPa.

2.3.2. Brazilian Test

On the other hand, the Brazilian test is an indirect tension test consisting in compressing a plain concrete cylinder placed horizontally by two steel plates (as shown in figure 4). On the models presented in the remainder of the paper, the effect of the plates on the top and bottom is accounted for by distributing the prescribed displacements on a contact zone following [19].

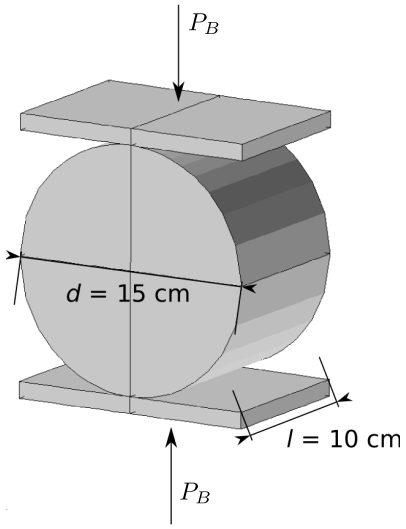

Figure 4: Description of the Brazilian test

For the Brazilian test, the relation between the tensile strength with the maximum vertical load is given by

$$f_t = \frac{2P_B}{\pi l d} \tag{7}$$

where l and d stand for the length and the diameter of the concrete specimen, respectively.

The given analytic expression is standard and there is agreement about its accuracy.

Experimentally, the average value obtained is $P_B = 8.6 \cdot 10^5$N, which is translated to the tensile strength, f_t, using the equation (7). Thus, the value of the tensile strength is set: $f_t = 3.84$MPa.

2.3.3. Experimental results

The data presented in table 1 is the result of an experimental campaign carried out in the *Departament d'Enginyeria de la Construcció* of the *Universitat Politècnica de Catalunya (UPC)*. The uniaxial compression test, the Brazilian test and the DPT are considered. The mean values are displayed and, in brackets, the coefficient of variation (standard deviation divided by the mean value) is presented. The Poisson ratio (ν) is assumed to be equal to 0.2.

Table 1: Experimental data

Description	Symbol	Value
Young's modulus	E	35.5GPa
Compressive strength (from the uniaxial compression test)	f_c	50.45MPa (2.69%)
Tensile strength (from the Brazilian test)	f_t	3.84MPa (8.36%)
Maximum load (from the DPT)	P	$1.52 \cdot 10^5$N (4.10%)
Vertical displacement at the maximum load (from the DPT)	u_z	$8.6 \cdot 10^{-4}$m (7.15%)

The DPT campaign consists in six test, three of them showed three fracture radial planes and the other three showed four fracture radial planes.

In this case, the uniaxial compression test (giving f_c), the Brazilian test (giving f_t as far as the Brazilian test is considered to be reliable) and the output of the DPT (the maximum vertical load P) are available for the same material. Numerical models are needed to find the expected value P of the DPT for a given f_t. Although analytically some expressions relating f_t and P for the DPT are available, they present scattering. The relation $f_t = \mathcal{F}_B(P_B)$

for the Brazilian test is reliable, therefore, the numerical models are validated firstly for this test.

3. Numerical modeling

Two different techniques are considered to simulate numerically the double punch test. On one hand, a continuous model, the nonlocal Mazars damage model (based on [15] and [1]), which has already been used in previous simulations of indirect tension tests [19]. On the other hand, a discontinuous model is considered based on introducing joint elements along the cracks. This model defines *a priori* the cracking pattern (known through the experimental tests and the analytical description of the DPT). Then, joint elements are used to model the cracks. The rest of the specimen is modeled as an elastic material.

The behavior of the DPT is a fully 3D phenomenon and, therefore, 3D modeling is required for both cases.

3.1. Nonlocal Mazars damage model

In a damage model, the constitutive equation is given by $\boldsymbol{\sigma} = (1-D)\mathbb{C}\boldsymbol{\varepsilon}$, where D is a scalar parameter representing the damage and obeying $0 \leq D \leq 1$. If $D = 0$, the material is considered healthy and if $D = 1$, the material is completely damaged. In the above, $\boldsymbol{\sigma}$ and $\boldsymbol{\varepsilon}$ stand for stress and strain tensor, respectively. Meanwhile, $\mathbb{C}$ is the elastic forth order tensor.

The damage parameter evolves depending on y, $D = D(y)$, which is called *state variable* and depends on the strain field, $y = y(\varepsilon)$. Commonly, the damage starts when the state variable reaches a given threshold Y_0 and it always increases.

The Mazars Damage Model considers the damage as a linear combination of the damage generated under tension, D_t, and the damage under compression, D_c,: $D = \alpha_t D_t + \alpha_c D_c$. Herein, the damage follows an exponential law and the state variable is defined as $y = \widehat{\varepsilon}$.

The Mazars damage model can be written as

$$D_t = 1 - \frac{Y_0(1-A_t)}{\widehat{\varepsilon}} - A_t e^{-B_t(\widehat{\varepsilon}-Y_0)} \qquad \alpha_t = \sum_i \frac{\varepsilon_{ti}\langle\varepsilon_i\rangle}{\widehat{\varepsilon}^2}$$

$$D_c = 1 - \frac{Y_0(1-A_c)}{\widehat{\varepsilon}} - A_c e^{-B_c(\widehat{\varepsilon}-Y_0)} \qquad \alpha_c = \sum_i \frac{\varepsilon_{ci}\langle\varepsilon_i\rangle}{\widehat{\varepsilon}^2}$$

with $\alpha_t + \alpha_c = 1$ and

$$\langle \varepsilon_i \rangle = \frac{\varepsilon_i + |\varepsilon_i|}{2} \qquad \widehat{\varepsilon} = \sqrt{\sum_i \left(\frac{\varepsilon_i + \mid \varepsilon_i \mid}{2} \right)^2}$$

where ε_i are the main strains.

Moreover, ε_{ti} and ε_{ci} are calculated following the next scheme:

$$\boldsymbol{\sigma} \rightarrow \boldsymbol{\sigma}_{prin} \begin{cases} \boldsymbol{\sigma}^+_{prin} \rightarrow \boldsymbol{\sigma}^+ \rightarrow \boldsymbol{\varepsilon}^+ \rightarrow \boldsymbol{\varepsilon}^+_{prin} \rightarrow \boldsymbol{\varepsilon}_{ti} \\ \\ \boldsymbol{\sigma}^-_{prin} \rightarrow \boldsymbol{\sigma}^- \rightarrow \boldsymbol{\varepsilon}^- \rightarrow \boldsymbol{\varepsilon}^-_{prin} \rightarrow \boldsymbol{\varepsilon}_{ci} \end{cases}$$

with $\boldsymbol{\sigma} = \boldsymbol{\sigma}^+ + \boldsymbol{\sigma}^-$ and $\boldsymbol{\varepsilon}_i = \boldsymbol{\varepsilon}_{ti} + \boldsymbol{\varepsilon}_{ci}$.

The parameters A_t, B_t, A_c, B_c and the threshold Y_0 are set depending on the material modeled, taking into account the relationship between damage parameters and experimental parameters.

The constitutive equation under tension for a uniaxial test can be written as

$$\sigma = \begin{cases} E \cdot \varepsilon, & \varepsilon \leq Y_0 \\ \\ \left[\dfrac{Y_0(1 - A_t)}{\varepsilon} + A_t \cdot e^{-B_t(\varepsilon - Y_0)} \right] \cdot E \cdot \varepsilon, & \varepsilon > Y_0 \end{cases} \tag{8}$$

and the constitutive equation under compression is deduced for a uniaxial test

$$\sigma = \begin{cases} E \cdot \varepsilon, & \varepsilon \leq Y_0 \\ \\ \left[\dfrac{Y_0(1 - A_c)}{\varepsilon} + A_c \cdot e^{-B_c(\varepsilon - Y_0)} \right] \cdot E \cdot \varepsilon, & \varepsilon > Y_0 \end{cases} \tag{9}$$

Now, the damage parameters deduction is presented based on (8) and (9).

- Imposing that *if* $\varepsilon = Y_0 \quad \Rightarrow \quad \sigma = f_t$ in (8), it results

$$Y_0 = \frac{f_t}{E} \tag{10}$$

- Under tension, $\lim_{\varepsilon \to \infty} \sigma = \sigma_\infty$, with σ_∞ standing for the residual tensile strength, is considered. Therefore, using (8),

$$E \cdot Y_0 \cdot (1 - A_t) = \sigma_\infty \quad \Rightarrow \quad A_t = 1 - \frac{\sigma_\infty}{E \cdot Y_0} \tag{11}$$

- $B_t = 10000 \cdot (1 + \xi)$, where ξ is a parameter measuring the material ductility.

- Under compression, $\sigma'(\varepsilon_{max}) = 0$. Let us derivate (9), getting

$$B_c = \frac{1}{\varepsilon_{max}} \tag{12}$$

- Imposing $\sigma(\varepsilon_{max}) = f_c$ under compression in (9) and using $B_c = \dfrac{1}{\varepsilon_{max}}$, A_c is obtained:

$$A_c = \frac{f_c - E \cdot Y_0}{-E \cdot Y_0 + E \cdot \varepsilon_{max} \cdot e^{(-1+\frac{Y_0}{\varepsilon_{max}})}} \tag{13}$$

- To ensure, under compression, that $0 \leq D \leq 1$ it is necessary to impose that

$$0 \leq A_c \leq 1 \tag{14}$$

In figure 5, the plain concrete damage model is presented in two graphics, one corresponding to the tension behavior (5(a)) and another to compression (5(b)).

Up to now, the damage has been calculated in each point depending on the state variable $y = \widehat{\varepsilon}$ at the same point, but this localization brings to a pathological mesh dependence and the results are not realistic. In order to solve this problem, a nonlocal damage model is considered, as introduced in [10]. The main idea of a nonlocal damage model is that the damage evolution depends on the state variable averaged in a neighborhood (associated to a characteristic length) of the current point, instead of depending on the state variable in the same point (as in a local model). Therefore a nonlocal state variable $\widetilde{y}$ is considered and it is defined as an average of the state

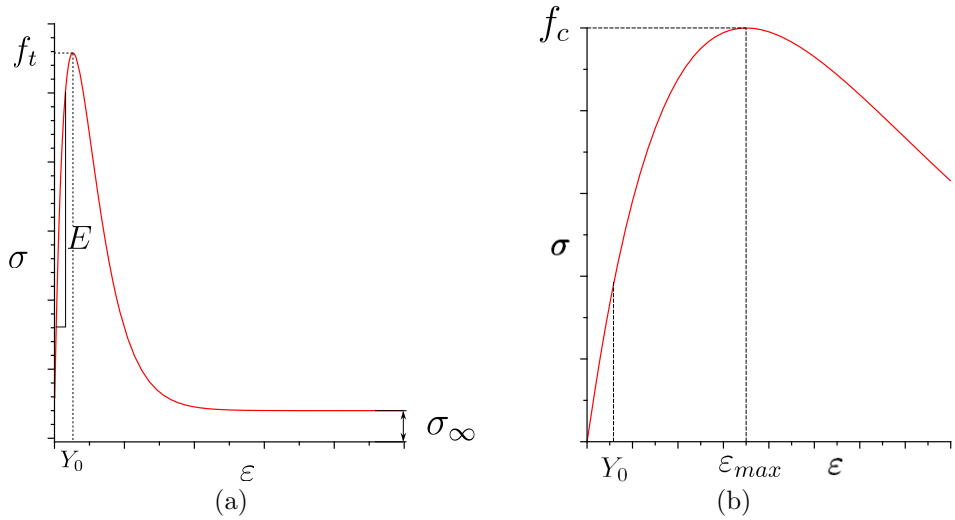

Figure 5: Uniaxial test. (a) Tension. (b) Compression.

variable in a neighborhood of each point. The characteristic length (l_{car}) is another material parameter and its function is to localize the nonlocality. In general, the value of the characteristic length is such that the neighborhood of each point involves two or three elements. Therefore, the nonlocal damage is $D = D(\widetilde{y})$. This is an integral nonlocal damage model because of the procedure employed for averaging the state variable, [18, 19].

3.2. Heuristic crack model with joints

An alternative to the damage model is a discontinuous model which considers the whole specimen as an elastic material and the cracking pattern defined using joint elements. In [13], all possible fracture paths are modeled using joint elements allowing any possible failure direction. Otherwise, in the double punch test, the cracking pattern is known *a priori*, therefore, only this cracking path is allowed (modeled using joint elements).

As introduced in [9], [2] and [20], the nodes in the interface zone must be defined twice in order to define the joint elements, which correspond to the duplicated geometry. Joint elements allow interfaces sliding and separating. The constitutive equations must incorporate both contact and noncontact conditions. When the interfaces are in contact, frictional sliding is possible, with dilatant behavior.

Any constitutive equation modeling a joint element in a three-dimensional

problem has three components. The first one corresponds to the normal direction of the joint plane and the other two are the tangential directions of the plane. The normal one corresponds to the contact or separation between the joint interfaces. Meanwhile, the ones in the joint plane correspond to the sliding directions.

The nonlinear behavior of joints is characterized by slide and separation taking place at the joint plane. For a joint with no tensile strength, separation of joint planes occurs when the tension normal to the joint plane becomes positive. Alternatively, a tensile strength can be given to the joint. If the shear strength of the joint is exceeded, irreversible slide occurs.

Herein, the Mohr-Coulomb Joint model is selected to model the collapse pattern of the double punch test. Therefore, the governing equations of the joint model can be written as

$$\sigma = k_{n1} \cdot u \quad \text{if} \quad \frac{-f_c}{k_{n1}} \leq u \leq u_0 \tag{15}$$

$$\sigma = (k_{n1} \cdot u_0 - k_{n2} \cdot u_0) + k_{n2} \cdot u \quad \text{if} \quad u \geq u_0 \tag{16}$$

$$\tau = -\tau_{max} \quad \text{if} \quad \frac{-\tau_{max}}{k_s} \leq v \tag{17}$$

$$\tau = k_s \cdot v \quad \text{if} \quad \mid v \mid \leq \mid \frac{\tau_{max}}{k_s} \mid \tag{18}$$

$$\tau = \tau_{max} \quad \text{if} \quad v \geq \frac{\tau_{max}}{k_s} \tag{19}$$

where $\tau_{max} = c + \sigma \tan(\varphi)$.

In equations (15)-(19), stresses applied are divided into two components (normal (σ) and shear (τ)), and the displacements are also divided into u and v, corresponding to σ and τ, respectively. Moreover, figure 6 reflects this constitutive law using two graphics: the normal (figure 6(a)) and shear (figure 6(b)) stresses.

In figure 7, it is shown (a) the relationship between stresses and displacements and (b) joint elements defined twice. There is a normal component and two shear components with the same behavior, but in an orthogonal direction.

The parameter deduction of the joint model is presented as follows: The first normal stiffness (N/m^3) is defined as $k_{n1} = \dfrac{E}{l}$, where l stands for the specimen height, as well as the shear stiffness, (N/m^3), $k_s = \dfrac{E}{l}$. Other-

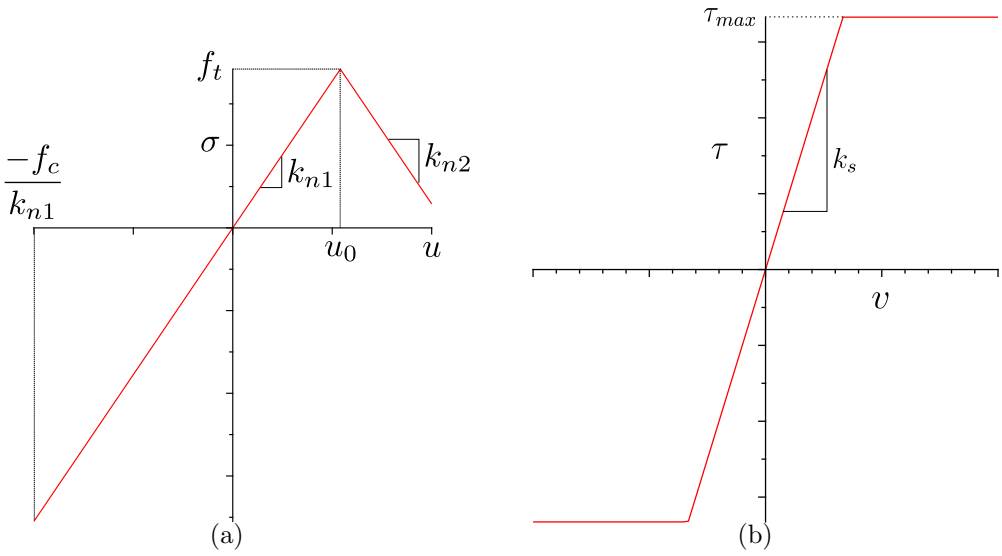

Figure 6: (a) σ and (b) τ evolution depending on the displacements for the joint model.

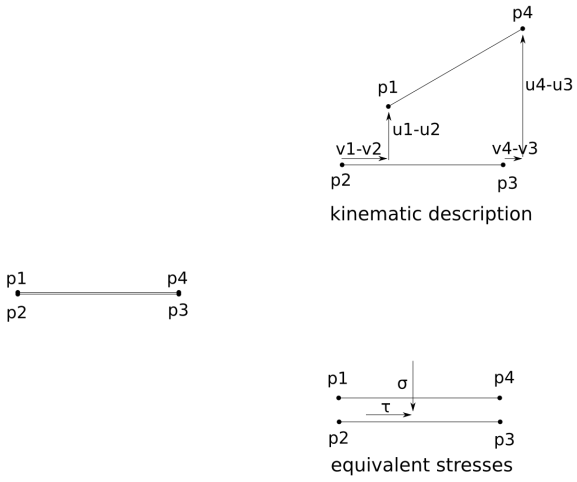

Figure 7: Stresses applied to a joint model and the corresponding displacements

wise, the second normal stiffness (N/m^3) must satisfy that $k_{n2} \leq 0$, because the negative branch is a modeling artifact to account for the sudden loss of strenght associated with cracking, while preserving the mathematical regu-

larity of the model. The threshold from k_{n1} to k_{n2} is defined as $u_0 = \dfrac{f_t}{k_{n1}}$ and the cohesion ($\mathrm{N/m^2}$) is $c = f_c$. Finally, the friction angle is fixed as $\varphi = 54°$, as found in the literature ([3]).

4. Numerical results and validation

All the results obtained considering both the continuous and the discontinuous model are presented. Both the Brazilian test and the double punch test are simulated. Moreover, the results are validated and compared with the analytical expressions and with the experimental data.

4.1. Nonlocal Mazars damage model

For simulating numerically considering the nonlocal Mazars damage model, six material parameters must be set: damage threshold (Y_0), characteristic length (l_{car}), tension parameters (A_t and B_t) and compression parameters (A_c and B_c).

From the experimental campaign, the value of the compressive strength obtained through the uniaxial compression test is available, $f_c = 50.45\mathrm{MPa}$. Therefore, through the uniaxial compression test, any parameter may be evaluated, but the relation between the two compression parameters is set. Hence, when A_c and B_c satisfy the given equation (13), the value of the compressive strength is set (f_c).

The value given by the experimental campaign from the Brazilian test is the tensile strength, $f_t = 3.84\mathrm{MPa}$. Therefore, through the equation (10), the value of Y_0 is set.

Hence, herein, some consideration must be taken into account:

- $Y_0 = \dfrac{f_t}{E} = \dfrac{3.84 \cdot 10^6}{35.5 \cdot 10^9} = 1.08 \cdot 10^{-4}$
- Considering any value of A_c satisfying $0 \leq A_c \leq 1$ is enough to ensure that $0 \leq D \leq 1$ and the chosen value does not influence on the results, therefore, $A_c = 1$.
- the relationship obtained from the uniaxial compression test between A_c and B_c must be satisfied (equation (13)), considering $f_c = 50.45\mathrm{MPa}$. Thus, $B_c = 266$.

- $A_t = 1 - \dfrac{\sigma_\infty}{E} = 1$, because the residual strength under tension is $\sigma_\infty = 0$ for plain concrete
- $B_t = 10000 \cdot (1 + \xi)$, with $0 < \xi < 1$, depending on the material. Hence, $B_t = 2500$, as appeared in [19].
- Observing the specimen size of the test and the expected fracture pattern, the caracteristic length (l_{car}) is set.

4.1.1. Brazilian test

Considering the previous information for simulating numerically the Brazilian test, the value of the tensile strength can be obtained (calculated through the value of the maximum vertical load, considering the equation (7)). All the material parameters are set previously, except l_{car} which depends on the fracture pattern of the test and its sizes. Therefore, l_{car} is set for obtaining the expected results. Hence, the optimal material parameters are presented in table 2.

Table 2: Optimal values of the material parameters of the nonlocal Mazars damage model for the Brazilian test

Material parameter	Value
Y_0	$1.08 \cdot 10^{-4}$
l_{car}	$2 \cdot 10^{-2}$m
A_t	1
B_t	2500
A_c	1
B_c	266

Vertical displacements are prescribed at the top of the specimen through one steel plate, which is modeled as an elastic material. Moreover, both horizontal and vertical symmetric conditions are imposed, thus, only a quarter of the specimen is taken into account during the whole simulation.

After the simulation, in figure 8, the value of the maximum vertical load depending on the vertical displacement is presented and, as expected, the maximum value is $P_B = 8.8 \cdot 10^5$N, which corresponds to $f_t = 3.74$MPa (considering the equation (7)).

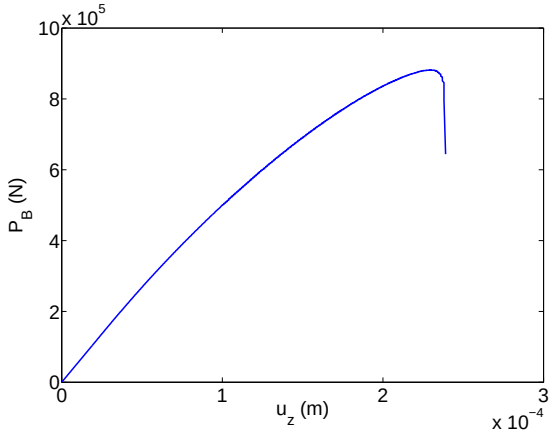

Figure 8: Brazilian test with the nonlocal Mazars damage model. u_z(m) - P_B(N).

In order to analyze the fracture pattern of the Brazilian test, the damage distribution obtained numerically is presented in figure 9.

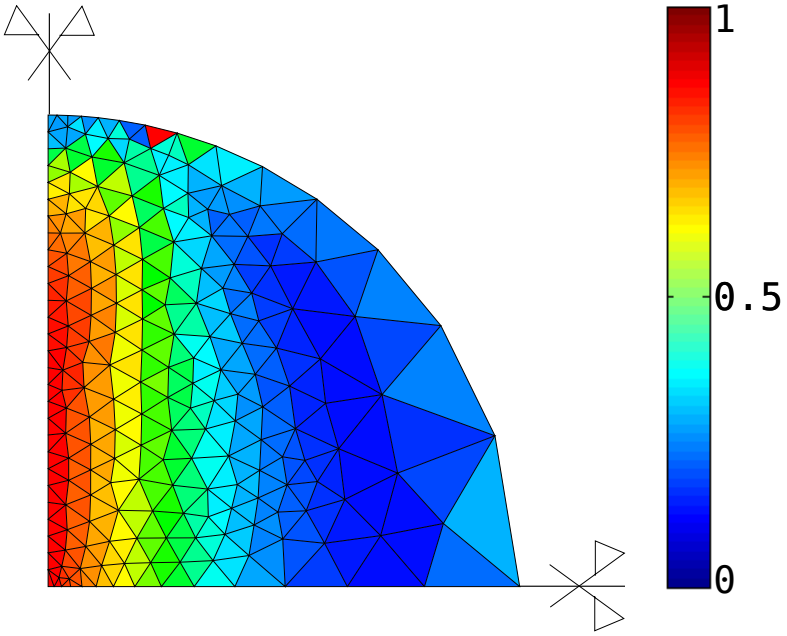

Figure 9: Damage distribution at the load peak

4.1.2. Double Punch Test

In this case, again, taking into account all the experimental information there is only one degree of freedom when setting the material parameters, l_{car}, which depends on the test size and the fracture pattern. l_{car} is set to adjust the numeric results with the experimental ones. Hence, the same parameter combination suitable for the Brazilian test is chosen, but with a different value of the characteristic length (as presented in table 3).

Table 3: Optimal values of the material parameters of the nonlocal Mazars damage model for the double punch test

Material parameter	Value
Y_0	$1.08 \cdot 10^{-4}$
l_{car}	$2.5 \cdot 10^{-3}$m
A_t	1
B_t	2500
A_c	1
B_c	266

Displacements are imposed at the top punch which are modeled as an elastic material. Symmetric conditions are imposed in order to work with half of the problem.

The vertical load versus the maximum vertical displacement is presented in figure 10. It is possible to observe that the maximum value ($1.92 \cdot 10^5$N) is close to the one obtained experimentally ($1.52 \cdot 10^5$N) and the vertical displacement value ($2.55 \cdot 10^{-4}$m) also is next to the experimental one. In addition, after the peak, it is possible to capture the behavior.

Figure 11 shows different views of the specimen with the damage distribution to be able to observe the whole cracking pattern. Looking at the damage distribution, four radial vertical cracking planes are observed (figures 11(a) and 11(b)). Moreover, the cone formation under the punch is presented, as expected, in the inside view of the specimen (figure 11(c)). Although the cracking pattern is detected, it is not possible to capture the whole pattern.

Although different meshes (for the same geometry) have been used with the numerical simulation of the double punch test considering the nonlocal Mazars damage model, the fracture pattern is always the same, as expected,

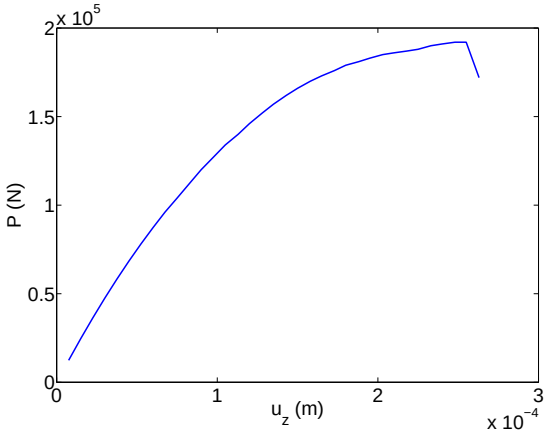

Figure 10: Double punch test with the nonlocal Mazars damage model. u_z(m) - P(N).

and placed as observed in figure 11, as well as the value of the maximum vertical load.

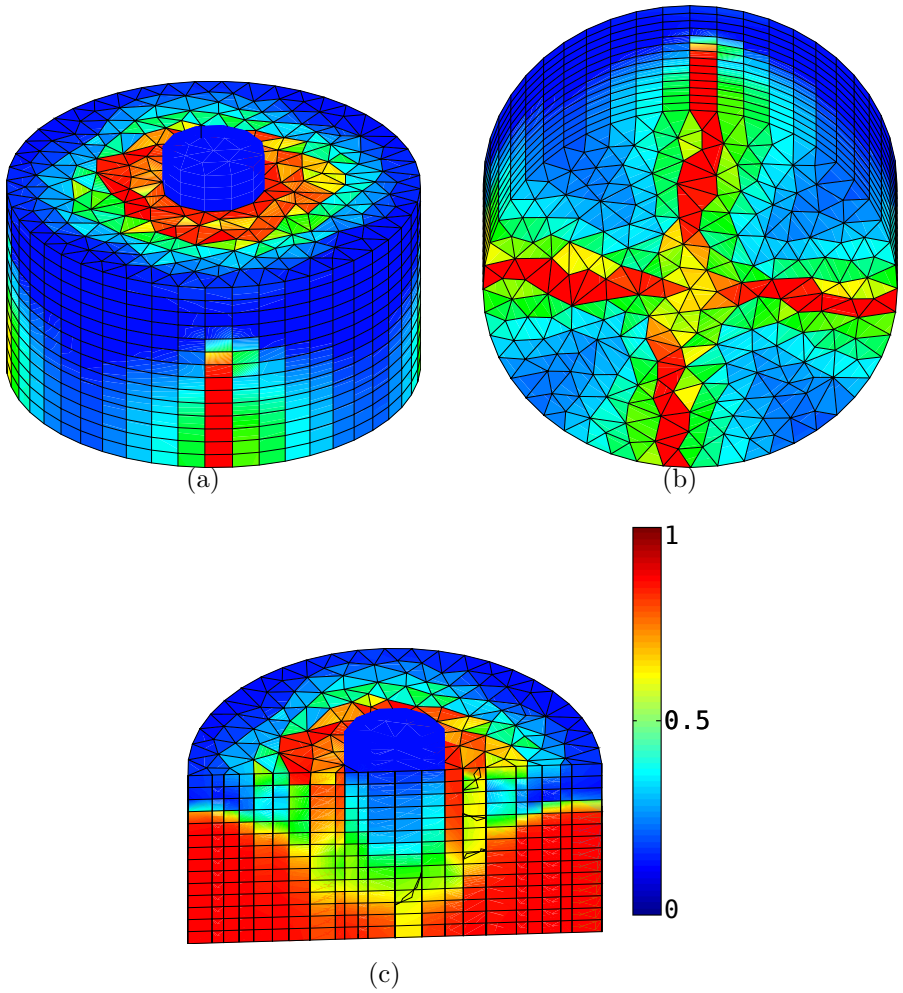

Figure 11: Damage distribution at the end of the simulation. (a) Top view. (b) Bottom view. (c) Inside view.

4.2. Heuristic model with joint elements in the cracking pattern

4.2.1. Brazilian test

Observing the damage distribution (figure 9), the Brazilian test is simulated modeling the cracking pattern with joint elements, meanwhile the rest of the specimen is considered elastic. In figure 12, joint elements are in red, meanwhile, the linear ones are in blue.

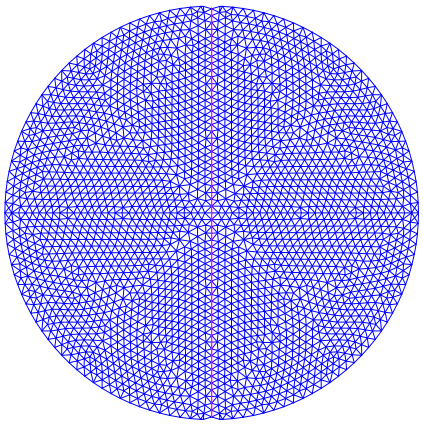

Figure 12: Brazilian test mesh for the discontinuous model

All the material parameters of the joint elements for the Brazilian test are set based on the experimental data ($f_t = 3.84$MPa and $f_c = 50.45$MPa) and the specimen height ($l = 0.1$m), as presented in table 4.

Vertical displacements are prescribed at the top and bottom sheets, modeled under an elastic model, and the whole specimen is taken into account.

Figure 13 presents the maximum vertical load (P_B) depending on the vertical displacement (u_z) and the maximum value of P_B is $P_B = 8.8 \cdot 10^5$N, which corresponds to $f_t = 3.72$MPa, considering the equation 7.

Table 4: Values of parameters for the Brazilian test

Symbol	Value
k_{n1}	$\frac{35.5 \cdot 10^9}{0.1}\mathrm{N/m^3}$
k_{n2}	$\frac{-35.5 \cdot 10^9}{0.1}\mathrm{N/m^3}$
u_0	$\frac{3.84 \cdot 10^6}{35.5 \cdot 10^9}\mathrm{m}$
k_s	$\frac{35.5 \cdot 10^9}{0.1}\mathrm{N/m^3}$
f_t	3.84MPa
c	50.45MPa
φ	54^o

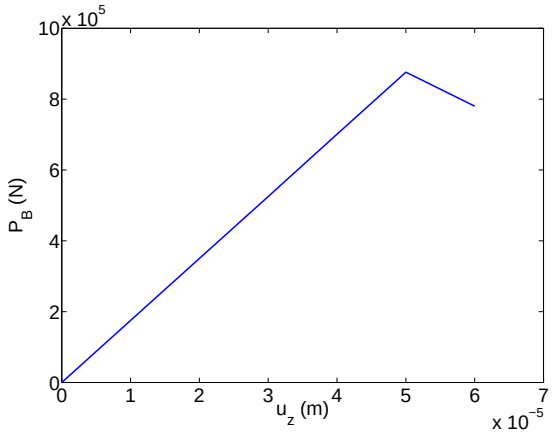

Figure 13: Brazilian test with the joint model. u_z(m) - P_B(N).

4.2.2. Double punch test

In order to simulate the double punch test considering the heuristic crack model with joint elements defined here, two different meshes are considered (as presented in figure 14): one with three radial planes and another with four radial planes.

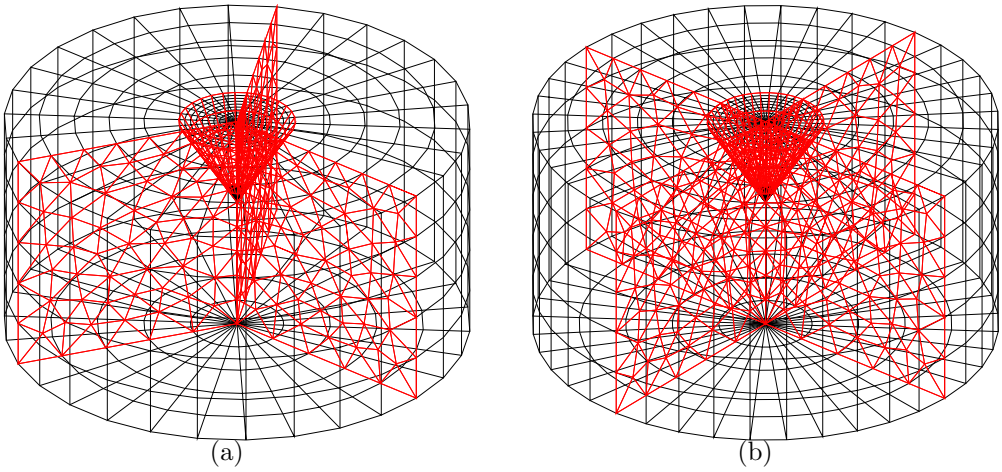

Figure 14: Double punch test including joint elements meshes. (a) three radial cracking planes. (b) four radial cracking planes.

Although double punch test is modeled in 3D, all joint elements are two-dimensional and triangular for the fracture planes and quadrilateral for the cone. The tip of the cone is not included in the mesh because it would be a point defined too many times. Besides, three auxiliary planes are defined corresponding to the specimen's cracking planes, but inside the cone. They are necessary to define properly the joint elements. For the case of four radial planes, also four auxiliary planes are defined inside the cone (corresponding to the intersection between the cone and the two diametral planes).

Firstly, three fracture radial planes are considered. All the material parameters are set using the experimental data and they are the same than for the Brazilian test, except the specimen height (herein, $l = 0.075$m) as presented in table 5. Moreover, the material parameters in the auxiliar joint elements inside the cone are defined in order to not influence on the results.

Vertical displacements are imposed at the top punch which is modeled as an elastic material. Horizontal symmetric condition is taken into account, thus, only half of the specimen is considered in the current simulation.

Table 5: Values of parameters for the Double Punch Test

Symbol	Value
k_{n1}	$\frac{35.5 \cdot 10^9}{0.075}$N/m^3
k_{n2}	$\frac{-35.5 \cdot 10^9}{0.075}$N/m^3
u_0	$\frac{3.84 \cdot 10^6}{35.5 \cdot 10^9}$m
k_s	$\frac{35.5 \cdot 10^9}{0.075}$N/m^3
f_t	3.84MPa
c	50.45MPa
φ	54^o

In figure 15, the maximum vertical load obtained is presented versus vertical displacement. As observed, it is possible to capture the behavior after reaching the peak load. The maximum vertical load ($1.55 \cdot 10^5$N) is in the same rang of values than the load obtained experimentally ($1.52 \cdot 10^5$N). Moreover, the value of the vertical displacements corresponding to the peak load ($5.25 \cdot 10^{-4}$m) is also close to the corresponding experimental value.

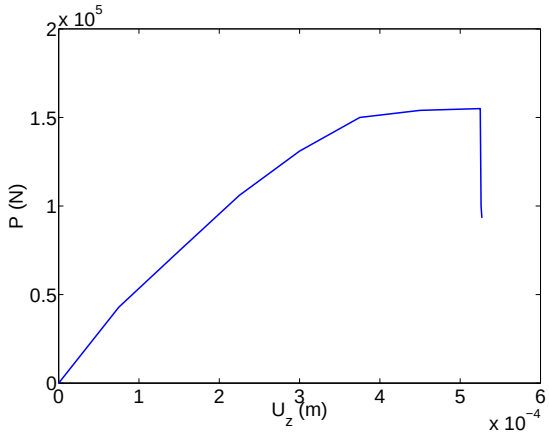

Figure 15: Double punch test modeled using joint elements considering three cracking planes. u_z(m) - P(N).

It is also observed that both the horizontal displacement (Δh) and the

vertical displacement (Δv), corresponding to the peak load, keep the same ratio than the relation between the two cathetus of the cone's generator triangle. That is, if the horizontal cathetus measures $c_h = 1.875$ cm and the vertical one, $c_v = 3$ cm, $\dfrac{c_h}{\Delta h} = \dfrac{c_v}{\Delta v}$ is satisfied.

Figure 16 represents the deformed mesh after the simulation from different points of views. The cone is penetrating the specimen, meanwhile the three cracking planes are opening in their normal directions.

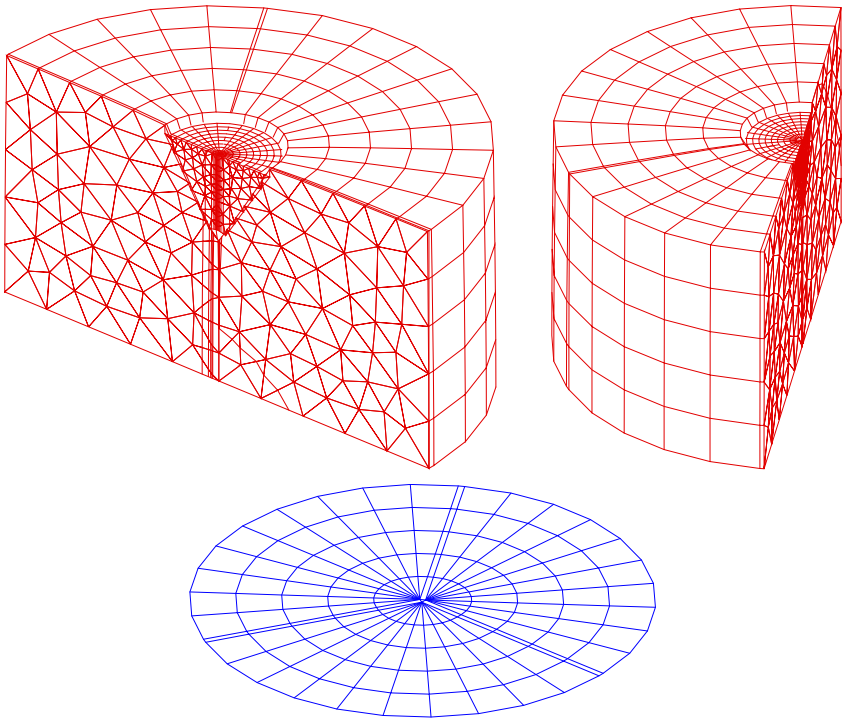

Figure 16: Double punch test modeled using joint elements considering three cracking planes. Deformed meshes amplified $\times 10$.

Once the results considering three cracking planes defined *a priori* are analyzed, four radial cracking planes are considered with the same material parameters (presented in table 5) than in the previous case. However, herein, the fracture pattern is different, so the same value of the maximum vertical load under the same conditions is not expected.

In figure 17 the results are presented and it is observed that the behavior is the same both with three and four radial cracking planes. Moreover, after the load peak, it is possible to obtain further results. Besides, the maximum vertical load ($1.56 \cdot 10^5$N) is still the same as the experimental value, and very close to the value obtained with three cracking planes. The value of the vertical displacement ($5.25 \cdot 10^{-4}$m) is also in the expected range of values.

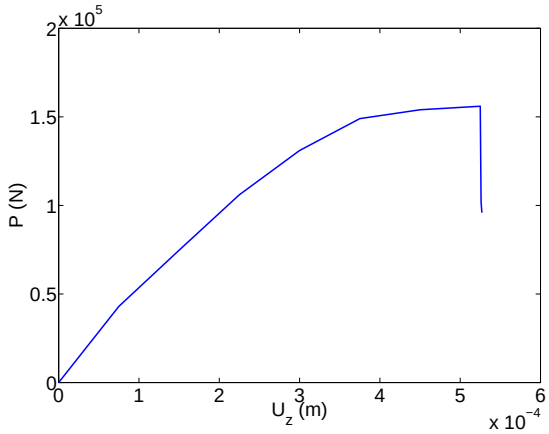

Figure 17: Double punch test modeled using joint elements considering four radial cracking planes. u_z(m) - P(N).

Once all the material parameters are set (for both cases, three and four radial fracture planes), a geometric parameter is studied: the cone's height. When defining *a priori* the fracture pattern, cone's height is an input. After considering different values of the cone height, it has been found that the value providing results in agreement with the experimental outcome is $h =$ 3cm. Note that this is also coinciding with the cone height observed in experiments.

4.3. Validation

Considering $f_c = 50.45$MPa and $f_t = 3.84$MPa set, in table 6 all the numerical results are presented and compared both with analytical expressions and experimental results.

- Analytical expressions:
  - $P_1 = f_t\pi(1.2l\dfrac{d}{2} - (\dfrac{d'}{2})^2)$, from [8].
  - $P_2 = \dfrac{f_t\pi(1.2l\dfrac{d}{2} - (\dfrac{d'}{2})^2)}{0.75}$, from [8].
  - $P_3 = f_t 9\pi l\dfrac{d'}{2}$, from [17].
- Experimental value: $P_{exp} = 1.52 \cdot 10^5$N

These values are compared to the numerical results considering the continuous model, P_{cont}, and the discontinuous one with three fracture radial planes, P_{disc3}, and four fracture radial planes, P_{disc4}.

The errors are computed considering $\text{Error}(P_i) = |\dfrac{P_i - P_j}{Pi}| \cdot 100\%$, being P_i the maximum vertical load obtained analytically or experimentally, and P_j the rest of the values.

Table 6: Model Validation

Description	P(N)	Error(P_1)	Error(P_2)	Error(P_3)	Error(P_{exp})
P_1	$1.51 \cdot 10^5$	0%	24.4%	4.1%	0.6%
P_2	$2.01 \cdot 10^5$	33.11%	0%	38.6%	32.2%
P_3	$1.45 \cdot 10^5$	3.4%	27.8%	0%	5%
P_{exp}	$1.52 \cdot 10^5$	0.6%	24.4%	5%	0%
P_{cont}	$1.92 \cdot 10^5$	27%	4.5%	32%	26.3%
P_{disc3}	$1.55 \cdot 10^5$	2.7%	22.9%	6.9%	2%
P_{disc4}	$1.56 \cdot 10^5$	3.3%	22.4%	7.6%	2.6%

5. Concluding remarks

To sum up, all the important conclusions of the present work are presented in the following.

The double punch test has been simulated using two different techniques: (a) the nonlocal Mazars damage model and (b) an elastic model considering the cracking pattern modeled with joint elements. In both cases, results are as expected, very close to the experimental and analytical ones (i.e. in the same range of values, as shown in table 6). These two numerical models are validated through the Brazilian test, taking into account the experimental information from the uniaxial compression test, the Brazilian test and the double punch test.

All the parameters (both the material and the geometrical ones) are set for both numerical models for each test. However, it is not proved that these material parameter combinations are unique. Experimental results are necessary to set all the parameters and, in general, the definition of the test.

After trying different material combinations for the nonlocal Mazars damage model, always taking into account all the conditions found during the present work, the optimal parameter combination is found. In this case, the only different parameter for the two different indirect tension tests (the Brazilian test and the double punch test) with the same concrete is the characteristic length which depends on the fracture pattern and the test size. Therefore, l_{car} is also seen as a numeric parameter which allows the numerical results fit with the experimental ones.

For the joint model, it is again observed that with a different fracture pattern (three or four planes), the same material parameters is used. Likewise, for the Brazilian test and the double punch test, except for the specimen height.

Compared with the available experimental results and some of the analytical expressions, the most suitable model is the discontinuous one considering both, three and four cracking radial planes because fits better the experimental results. However, using the joint model, it is necessary to know the fracture pattern before the simulation. Meanwhile, with the nonlocal Mazars damage model, the failure pattern is not set *a priori*. Moreover, the fracture pattern obtained considering the damage model fits with the experimental one and the obtained peak value corresponds to other analytical expressions.

Time calculation and computational cost are shorter using the discontinuous model than with the nonlocal Mazars damage model, due to the number

of nonlinear elements in each model.

Both the nonlocal Mazars damage model and the model including joint elements in the cracking pattern are valid alternatives to simulate the double punch test, which was designed for studying the tensile strength (f_t) of concrete. Therefore, these numerical simulations allow to control f_t, for any material parameters considering both models. In both cases, f_t is an input of the problem and the maximum vertical load, P, is the output of the problem.

Having at hard these two alternatives allows reproducing numerically the behavior of the DPT described by different authors and also with experimental results available.

Up to now, the double punch test has been simulated numerically for plain concrete. Then the next step is including fibers into these models in order to simulate the double punch test for steel fiber reinforced concrete (a test introduced in [17] and [16], defined as the *Barcelona Test*).

Acknowledgements

Authors gratefully acknowledge the financial support of the Ministerio de Fomento, ayudas a la construcción 2006 (project number C 59/2006), and the Ministerio de Ciencia e Innovación (project DPI2007-62395).

References

[1] Z. P. Bažant. "Concrete fracture models: testing and practice". *Engineering Fracture Mechanics.*, Vol. **69**, 165-205, 2002.

[2] G. Beer. "An isoparametric joint/interface element for finite element analysis". *International Journal For Numerical Methods in Engineering.*, Vol. **21**, 585-600, 1985.

[3] L. Bortolotti. "Double-punch test for tensile and compressive strengths in concrete". *IACI Materials Journal.*, Vol. **85-M4**, 26-32, 1988.

[4] K. T. Chau, X. X. Wei. "Finite solid circular cylinders subjected to arbitrary surface load. Part I: Analytic solution". *International Journal of Solids and Structures.*, Vol. **37**, 5707-5732, 2000.

[5] K. T. Chau, X. X. Wei. "Finite solid circular cylinders subjected to arbitrary surface load. Part II: Application to double-punch test". *International Journal of Solids and Structures.*, Vol. **37**, 5733-5744, 2000.

[6] W. F. Chen. "Double punch test for tensile strength of concrete". *ACI Mater J.*, Vol. **67 (2)**, 993-995, 1970.

[7] W. F. Chen, B. E. Ttumbauer. "Double-punch test and tensile strength of concrete". *Journal of Materials, American Society of testing and materials.*, Vol. **7 (2)**, 148-154, 1972.

[8] W. F. Chen, R. L. Yuan. "Tensile strength of concrete: Double punch test". *Journal of structural divisions, ASCE.*, Vol. **106**, 1673-1693, 1980.

[9] P. Díez, P. Pegon. "Error assessment of structural computations including joints". *Proceedings of the Fifth World Congress on Computational Mechanics.*, Vienna, Austria. July 7-12, 2002.

[10] M. Jirásek. "Nonlocal damage mechanics". *Damage and fracture in geomaterials.*, Vol. **11**, 993-1021, 2007.

[11] G. Lilliu, J. G. M. Van Mier. "3D lattice type fracture model for concrete". *Engineering Fracture Mechanics.*, Vol. **70**, 927-941, 2003.

[12] G. Lilliu, J. G. M. Van Mier. "Analysis of crack growth in the Brazilian Test, in construction materials -theory and application". *Eligehausen R. (Ed.) H. W. Reinhardt 60th birthday commemorative volume*, 123-138, Stutgart, Novembre 1999.

[13] C. M. López, I. Carol, A. Aguado. "Estudio de la fractura del hormigón mediante un modelo numérico micromecánico con elementos junta". *MECOM 99.*, Mendoza, Argentina. September 6-10, 1999.

[14] P. Marti. "Size effect in double-punch test on concrete cylinders". *ACI Materials Journal.*, Vol. **86-M58**, 597-601, 1989.

[15] J. Mazars. "A description of micro- and macroscale damage of concrete structures". *Engineering Fracture Mechanics*, Vol. **25**, 729-737, 1986.

[16] C. Molins, A. Aguado, S. Saludes. "Double Punch Test to control the energy dissipation in tension of FRC (Barcelona Test)". *Materials and Structures.*, Vol. **42**, 415-425, 2009.

[17] C. Molins, A. Aguado, S. Saludes, T. Garcia. "New test to control tension properties of FRC". *ECCOMAS Thematic Conference on Computational Methods in Tunnelling (EURO:TUN 2007).*, Vienna, Austria, August 27-29, 2007.

[18] G. Pijaudier-Cabot, A. Huerta. "Finite element analysis of bifurcation in nonlocal strain softening solids". *Computer Methods in Applied Mechanics and Engineering.*, Vol. **90**, 905-919, 1991.

[19] A. Rodriguez-Ferran, A. Huerta. "Error estimation and adaptivity for nonlocal damage models". *International Journal of Solids and Structures.*, Vol. **37**, 7501-7528, 2000.

[20] M. F. Snyman, W. W. Bird, J. B. Martin. "A simple formulation of a dilatant joint element governed by Coulomb friction". *Engineering Computations.*, Vol. **8**, 215-229, 1991.